A large-scale 3d computer tomography analysis of primary dendrite arm spacing response to withdrawal velocity change using dendrite centre tracking

Miller, Joshua; Sturz, Laszlo; Steinbach, Sonja; Zimmermann, Gerhard; Warnken, Nils

A Large-Scale 3D Computer Tomography analysis of Primary Dendrite Arm Spacing Response to Withdrawal Velocity Change Using Dendrite Centre Tracking

Miller, Joshua; Sturz, Laszlo; Steinbach, Sonja; Zimmermann, Gerhard; Warnken, Nils

A Large-Scale 3D Computer Tomography analysis of Primary Dendrite Arm Spacing Response to Withdrawal Velocity Change Using Dendrite Centre Tracking

J. E. Miller[1], L. Sturz[2], S. Steinbach[3], G. Zimmermann[2], and N. Warnken[1]

[1]Department of Metallurgy and Materials, University of Birmingham, United Kingdom, B15 2TT

[2] ACCESS e.V., Intzestr. 5, 52072 Aachen, Germany

[3] Institut für Materialphysik im Weltraum, Deutsches Zentrum für Luft- und Raumfahrt (DLR), 51170 Köln, Germany

Email of corresponding author: N.Warnken@bham.ac.uk

Keywords: Directional Solidification; Computerised Tomography; Primary Dendrite Arm Spacing; Changing Withdrawal Velocities; 3D Metallography; Dendrite Centre Tracking; Aluminium 10 wt% Copper

Abstract. Directional solidification of alloys is an extremely important process to understand due to the many high value products that are produced in this manner, *e.g.* turbine blades. Controlling how the columnar dendrites grow and pack together is an important aspect of increasing the strength and longevity of these components. As such 3D examination of a 200 mm in length and 6 mm diameter aluminium 10 wt % copper rod solidified under varying withdrawal rates (40 μm/s then a jump to 80 μm/s) has been undertaken in a lab based computerised tomography (*CT*) machine. Novel image analysis techniques involving active contours and skeletonisation have been used to track the dendrites through the sample itself. Sites of dendrite initiation and termination have been identified automatically within the dataset. These points of dendrite creation or deletion where found to be most prevalent after a step change in the withdrawal rate. Information on the array packing and primary dendrite arm spacing (*PDAS*, λ) for each grain within the sample has been obtained. The results show that there is a distance delay after the withdrawal rate change and the onset of a *PDAS* restructuring.

Introduction

With the advent of lab based computerised tomography (*CT)* scanners there has been an increase in the options available for 3D metallography that researchers can undertake. *CT* scanners allow for the non-destructive analysis of components and castings and can build up a 3D virtual view of the internal microstructure of a component. This has allowed for the quick and relatively easy evaluation of microstructures in three dimensions where previously the only avenue available to researchers was the use of tedious serial sectioning.

Moreover with the increase of computation power available greater volumes of data can be now analysed swiftly and cost effectively. As such now is the first time that the large volumes associated with *CT* analysis can be effectively analysed and giving a greater understanding of how a dendritic array evolves in a directionally solidified sample giving a stable *PDAS.*

Many equations for *PDAS* calculation have been put forward including the Trivedi equation which takes account of the marginal stability criterion [1]:

$$\lambda = 2.83\, m(k-1)D\Gamma LC^{0.25}v^{-0.25}G^{-0.5} \qquad (1)$$

Where: m is the liquidus slope [K/wt%]; k is the partition coefficient; D is the diffusivity of solute in the liquid [m^2s^{-1}]; Γ is the Gibbs-Thomson coefficient [mK]; L is a constant which depends upon the harmonic perturbations which is set to 28 [1]; C is the bulk composition [wt%]; v is the solidification front velocity; and G is the thermal gradient [K/m].

Eq. 1 has proven adapt in producing predictions for the *PDAS* in steady state solidification. However not quite as adapt in the unsteady state. In this type of situation, the dendritic array restructures to compensate for changing solidification conditions resulting in either the creation or termination of primary dendrite arms [2-5]. Ma [2 & 3] set the stable limit for the *PDAS* to $\lambda_{min} = 2/3\ \lambda$ to $\lambda_{max} = 4/3\ \lambda$. If the *PDAS* becomes too small a dendrite is outcompeted and killed off and the microstructure readjusts increasing the *PDAS*. Conversely if the *PDAS* is too large then a new primary dendrite arm will fill a gap in the array formed from the growth of a tertiary arm from one of the surrounding dendrites.

This array restructuring is easy to see in two dimensional samples especially in transparent model alloys [2-4]. However, it is much more difficult in 3D. When calculating the *PDAS* in a solidified sample it must first be sectioned and the number of individual dendrites (N) counted, then using the equation:

$$\lambda_B = \sqrt{\frac{A}{N}} \qquad (2)$$

the bulk *PDAS* can be calculated for that transverse section of the sample if the area of the slice, A, is known [6-8]. The drawback of this method is that it only gives an average value for the *PDAS* so no statistical analysis can be undertaken using it. Methods such as the Warnken-Reed and Voronoi *PDAS* calculations can however be used to find the local *PDAS* across a sample [6-8].

Therefore, in order to test how microstructures readapt in 3D to changing solidification conditions, an Al-10 wt% Cu sample was directionally solidified under a constant *G* of 10 K/m with an instantaneous velocity jump from 40 μm/s to 80 μm/s. It was then imaged in a *CT* and examined using custom algorithms developed by the authors in Matlab to calculate the local and bulk *PDAS* and find instances where new dendrites are created.

Methodology

An Al-10wt% Cu master alloy billet was cast from commercially pure aluminium and copper at the University of Birmingham Casting lab. It was then *EDM*ed into a 200 mm length rod with a 6 mm diameter in the Netshape Laboratory, Birmingham. The sample was then directionally solidified in the lab-scale CARLO Bridgman furnace at ACCESS e.V. Germany under a constant withdrawal of 40 μm/s for 60 mm with an instantaneous velocity jump to 80 μm/s which was then constant for 30 mm. The bottom 90 mm of the sample was used to hold the sample in place and top 20 mm was assumed to be unusable. These lengths for the 40 and 80 μm/s sections were chosen to give each section an equal number of diffusion lengths ($800L_d$ in each instance) for the usable 90 mm of sample where: $L_d = D/v$. Which is an L_d of 75 μm and 37.5 μm respectively (using parameters in Table 1).

The sample was then *CT*ed at the Institut für Materialphysik im Weltraum at the German Aerospace Centre (DLR), using a GE Phoenix nanotom microCT scanner with an acceleration voltage of 100 kV and a current of 110 μA. The resulting voxel size was 2 μm^3. The images were then analysed using a series of author written applications within Matlab to: binarise and segment the images using active contours; then find the centre of each dendrite using the skeleton centre method [9]. The dendrite centres of each slice were then joined up forming lines that followed the primary arm of a dendrite producing a “forest” of separate dendrite trunks. The coordinates of a newly initiated dendrite were found by locating where these traced lines branched. This branching indicates a situation where a tertiary arm from the original primary trunk has become stable and formed a new primary trunk.

The bulk *PDAS* for each slice in the sample was calculated using equation 2 above. The local *PDAS* along the length was also calculated using the Voronoi and Warnken-Reed methods which are described by Tschopp et al. [6 & 7] and Warnken and Reed [8]. The average number of nearest neighbours for these two methods was also calculated. In the Warnken-Reed method the authors used an α value of 1.5. The results of this were compared with calculations for the *PDAS* using Eq. 1 and the parameters given in Table 1.

Table 1: Table of parameters used in Eq. 1 to calculate the PDAS [10]

Parameter	Value
C	10 [wt% Cu]
D	$3x10^{-9}$ [m^2s^{-1}]
G	10 000 [Km^{-1}]
k	0.14
L	28
m	-3.37 [$Kwt\%^{-1}$]
v_1	40 [μms^{-1}]
v_2	80 [μms^{-1}]
Γ	2.41 [Km]

Results

The *PDAS* was determined along the length of the manipulated and binarised *CT* volume (Fig. 1, with two of the *CT* slices before and after the transition shown in Fig. 2) using each of the different methods described above *i.e.* the bulk, Warnken-Reed, and Voronoi. As can be seen in Figure 1 the bulk *PDAS* method gives the highest value for the *PDAS* along the sample with the Voronoi and then Warnken-Reed below that. The evolving dendrite array takes approximately 2500 μm (equivalent to 66 L_d) until the *PDAS* stabilises and does not decrease further. After which it remains relatively constant. The minimum and maximum stable *PDAS* has also been calculated and shown on Fig. 1. These values were calculated for each slice using $\lambda_{min} = 2/3\ \lambda$ to $\lambda_{max} = 4/3\ \lambda$.

Fig. 3 shows that along the length of the sample there was a slight increase in the number of nearest neighbours in the Warnken-Reed method on the order of 0.05 neighbours. Whereas the Voronoi method shows an increase of approximately 0.2 new neighbours. In both instances there is a steady increase after the velocity change until it plateaus after 2500 μm.

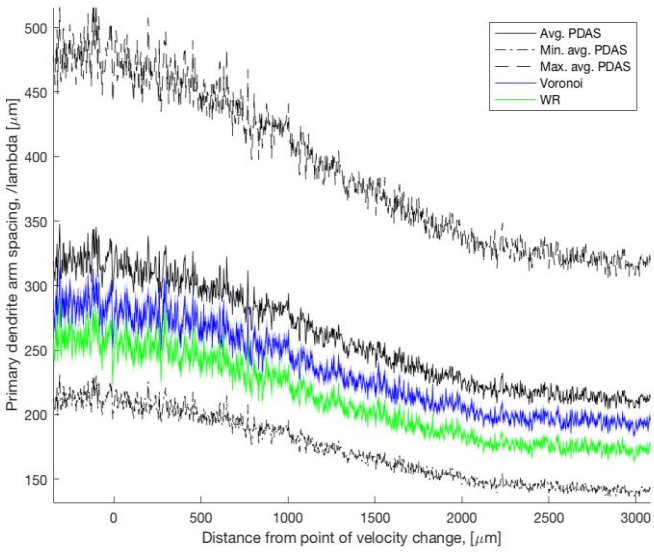

Figure 1: PDAS along the length of the sample from the velocity change

Fig. 4 shows the cumulative number of created or outcompeted dendrites along the length of the sample. As can be seen there is a relatively constant rise in the number of new dendrites being formed after the velocity change. Whereas after 1000 μm there begins to be dendrites which are eliminated.

The calculated values for the *PDAS* using Eq. 1 and the parameters in Table 1 were 310 μm and 260 μm at 40 μm/s and 80 μm/s respectively. The former value shows good agreement with the results in Fig. 1 prior to the velocity change (distance < 0 μm). Whereas the calculated value for the PDAS of 260 μm at 80 μm/s (distance > 2500 μm) is incorrect by 40 μm as

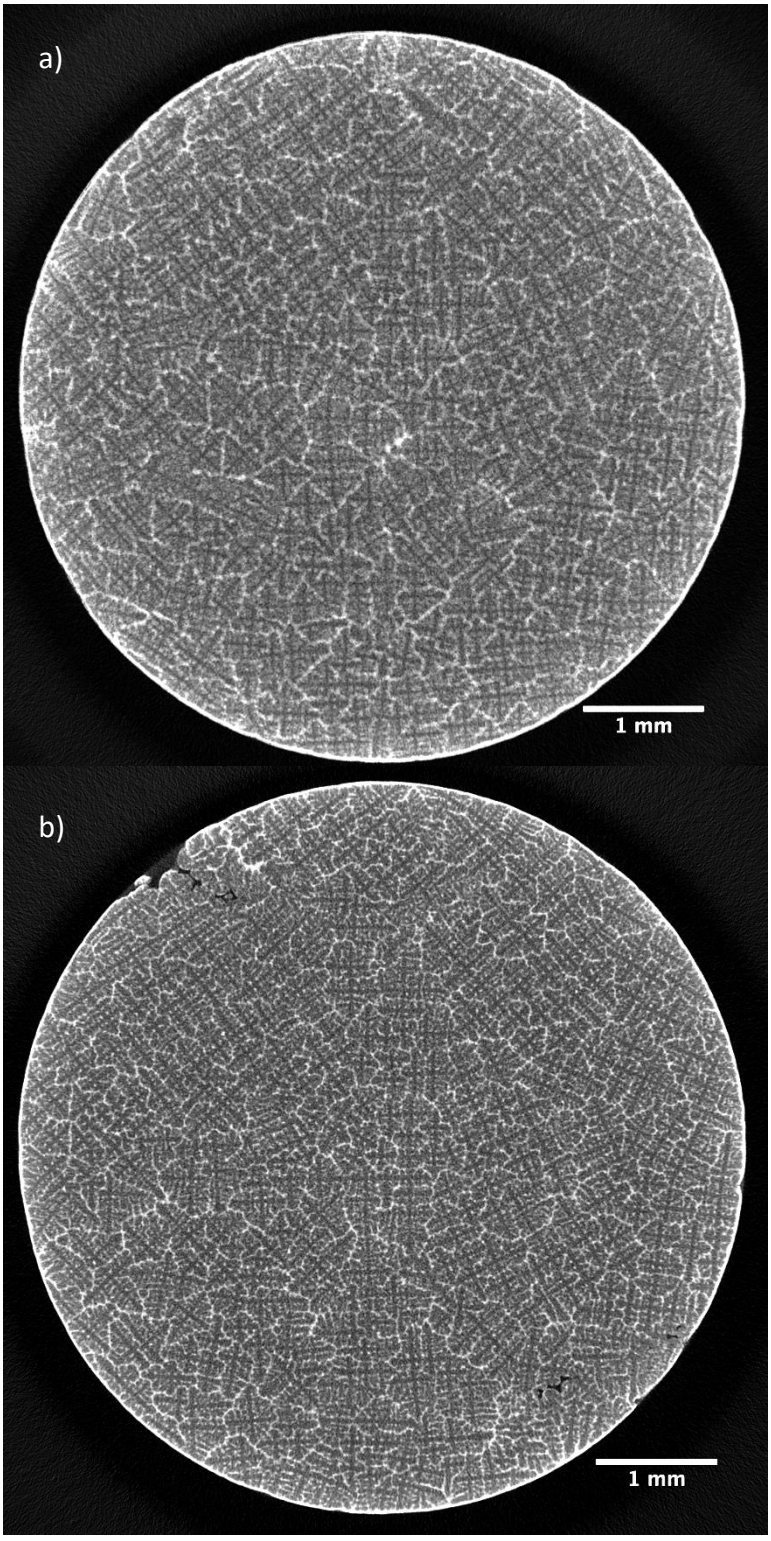

Figure 2: CT micrographs of the sample 1 mm before the velocity change (a) and 3 mm after the transition (b)

the stabilised PDAS in this region is 220 μm. However Eq. 1 is just one of many *PDAS* calculation models.

Using information from Fig. 4 the location of the initiations and deletions was found. Fig. 5 shows the stabilisation and deletion of dendrites within the array after 1700 μm and every 200 μm afterwards until 2300 μm. In both cases of stabilisation and deletion the dendritic array readjusts itself around the new or removed dendrite.

Discussion

The results of the experiment show that the microstructural array rearranges itself with changing solidification conditions. In this instance, an increase in the velocity from 40 to 80 μm/s. The *PDAS* decreased when calculated using Eq. 2, and with the Voronoi and Warnken-Reed methods for each slice along the length of the sample. This reduction in *PDAS* was expected due to the expectation that the evolving microstructural array would adapt to a lower value (as shown by comparing Fig. 2a and 2b). This re-adaption was achieved by means of a production of new primary dendrite trunks which formed from the stabilisation of tertiary dendrite arms (Fig. 5). As can be seen in Fig. 4 there is a continual increase in the number of new primary dendrite arms after the velocity change. Including after this graph shows that the dendrite array restructuring was not due to a columnar to equiaxed transition (*CET*) but rather a gradual restructuring as new tertiary dendrite arms fill gaps within the dendritic array.

Moreover Fig. 4 and 5 show that there are some instances of dendrites being out competed and "killed off". The last such instance of a dendrite being out competed coincides with the levelling off in the number of nearest neighbours seen in Fig. 3. After this levelling of the *PDAS* remains constant and so too does the approximate number of total dendrites.

Fig. 5 also implies that the missorientation between the dendrites may play a role in the deletion of the dendrites. The outcompeted dendrite is missorientated by 45° to all the surrounding nearest neighbours.

A clear feature of Fig. 1 is that the *PDAS* adjustment is not an instantaneous process but takes place over several mm. In this instance, approximately 2.5 mm. This distance corresponds to approximately 70 times the diffusion length in the 80 μm/s regime. It is possible that the diffusion length L_d plays an intrinsic part in the restructuring of a dendritic microstructure. As it may be possible that a certain number of L_d need to be reached before the array reaches a stable and unchanging *PDAS* after a velocity change. However more experiments will need to be undertaken to see if this or another parameter plays a role in the time taken for a dendritic array to re-stabilise.

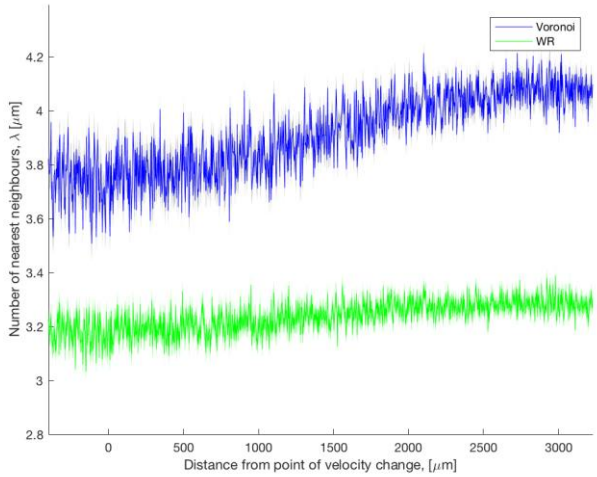

Figure 3: Change in nearest neighbour number along the length of the sample

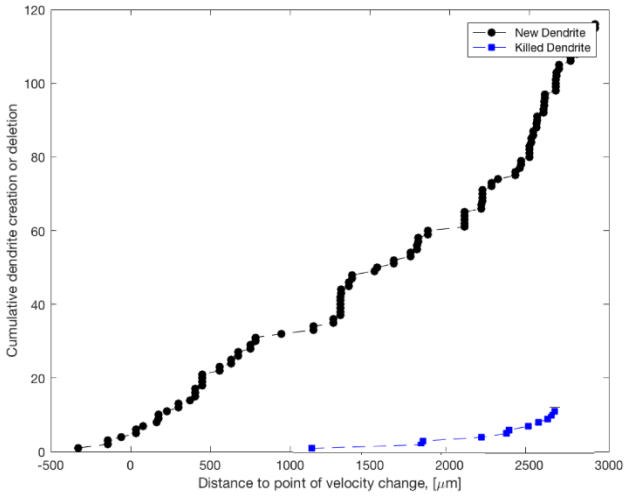

Figure 4: Cumulative dendrite creation or deletion along the length of the sample

Conclusions

A directionally solidified Al-10 wt% Cu rod was solidified under a 40 μm/s withdrawal rate which was instantaneously changed to 80 μm/s after 60 mm. This was achieved to promote dendritic array restructuring by the promotion of tertiary arms stabilising into primary arms.

The solidified rod was *CT*ed and analysed using image analysis algorithms written by the authors to trace the centre of the dendrites using the Skeleton Centre method [9]. The *PDAS* was calculated along the length of the sample using the bulk, Voronoi, and Warnken-Reed methods showing in each case that it took approximately 2.5 mm for the array structure to return to steady state with a continuous *PDAS*.

During this transition, new dendrites were created via the promotion of tertiary arm growth and tracked within the 3D *CT* volume. The creation of these new primary arms gives credence to the extension of 2D dendrite array restructuring [2-5] in 3D. Moreover, sites where primary trunks were out competed were also found along the length of the sample showing that the microstructure is continuously adjusting the array to bring it into a stable configuration.

The authors tentatively put forward that the diffusion length L_d may in some way be used to predict the length that the array adjustment occurs over until a new stable *PDAS* is reached. For this sample, approximately 66 L_d at 80 μm/s were reached before the array stabilised at a *PDAS* of 230 μm.

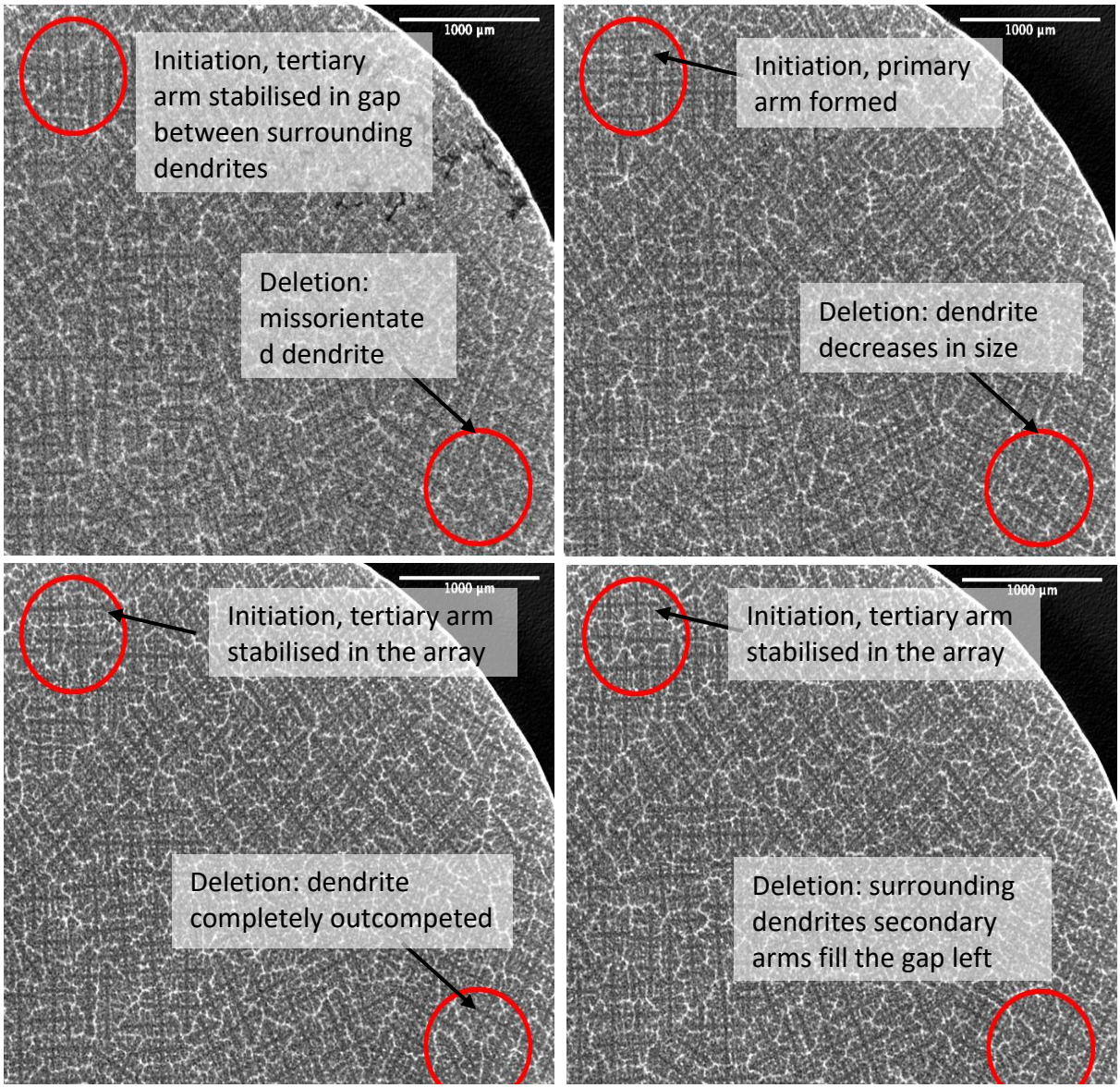

Figure 5: Sites of dendrite initiation and deletion. The images are a) 1700 µm b) 1900 µm, c) 2100 µm and d) 2300 µm from the velocity change.

Acknowledgments

This work forms part of the Microstructure Formation in Casting of Technical Alloys under Diffusive and Magnetically Controlled Conditions (MICAST) project. The authors would like to thank the ESA for funding as part of the MICAST project and support with this work. With special thanks to Adrian Caden and Peter Cranmer for help casting the master alloy; Amanda Field and Sam Crutchely for the help with EDMing the sample; Christoph Pickmann at Acces e.V. for running the Bridgman furnace; and Vanessa Indrizzi for help with the Matlab code.

References

[1] R. Trivedi. Interdendritic spacing: Part ii. a comparison of theory and experiment. Metallurgical and Materials Transactions A, 15(6):977–982, Jun 1984.

[2] D. Ma. Development of dendrite array growth during alternately changing solidificaton condition. Journal of Crystal Growth, 260:580–589, 2004.

[3] D. Ma. Response of primary dendrite spacing to varying temperature gradient during directional solidification. Metallurgical and Materials Transactions B, 35B:735–742, 2004.

[4] E. Üstün, E. Çadirli, and H. Kaya. Dendritic solidification and characterization of a succinonitrile–acetone alloy. Journal of Physics: Condensed Matter, 18(32):7825, 2006.

[5] V. Indrizzi, N. Warnken, and D. Putman. Computational study of spacing selection in directionally growing dendritic arrays. In SP17, 07 2017.

[6] M. A. Tschopp, J. D. Miller, A. L. Oppedal, and K. N. Solanki. Characterizing the local primary dendrite arm spacing in directionally solidified dendritic microstructures. Metallurgical and Materials Transactions A, 45(1):426–437, 2014.

[7] M. A. Tschopp, J. D. Miller, A. L. Oppedal, and K. N. Solanki. Evaluating local primary dendrite arm spacing characterization techniques using synthetic evaluating local primary dendrite arm spacing characterization techniques using synthetic directionally solidified dendritic microstructures. Metallurgical and Materials Transactions A, 46A:4610–4628, October 2015.

[8] N. Warnken and R. C. Reed. On the characterization of directionally solidified dendritic microstructures. Metallurgical and Materials Transactions A, 42(6):1675–1683, 2011.

[9] J. E. Miller, M. Strangwood, S. Steinbach, and N. Warnken. Skeletonisation to find the centre of dendrites traced from a 2d microstructural image. In Z. Fan, editor, Solidification Processing 2017, 2017.

[10] M. Gündüz and E. Çadrli. Directional solidification of aluminium–copper alloys. Materials Science and Engineering: A, 327(2):167 – 185, 2002.